ISSN 2072-5981

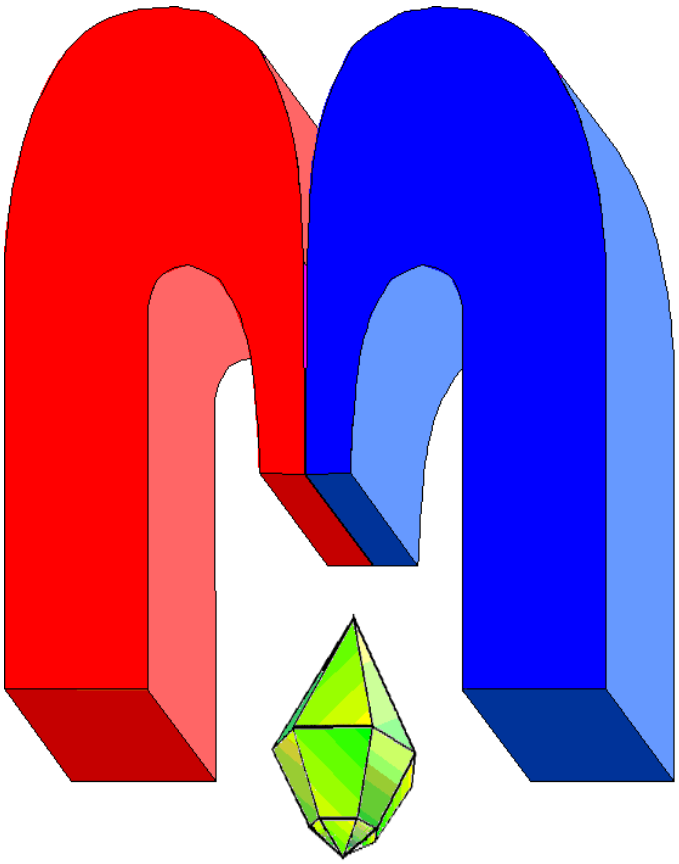

Magnetic Resonance in Solids

Electronic Journal

Volume ***21,***
Issue ***2***
Paper No ***19204,***
1-7 pages
2019

http://mrsej.kpfu.ru
http://mrsej.ksu.ru

Established and published by Kazan University
Endorsed by International Society of Magnetic Resonance (ISMAR)
Registered by Russian Federation Committee on Press (#015140), August 2, 1996
First Issue appeared on July 25, 1997

"***Magnetic Resonance in Solids. Electronic Journal***" (**MRS*ej***) is a peer-reviewed, all electronic journal, publishing articles which meet the highest standards of scientific quality in the field of basic research of a magnetic resonance in solids and related phenomena.

Indexed and abstracted by
Web of Science (*ESCI*, Clarivate Analytics, from 2015), *Scopus* (Elsevier, from 2012), *RusIndexSC* (*eLibrary*, from 2006), *Google Scholar*, *DOAJ*, *ROAD*, *CyberLeninka* (from 2006), *SCImago Journal & Country Rank*, etc.

* In Kazan University the Electron Paramagnetic Resonance (EPR) was discovered by Zavoisky E.K. in 1944.

High frequency EPR spectroscopy of Er^{3+} ions in $LiYF_4$ and $LiLuF_4$: a case study of crystal fields

G.S. Shakurov[1,*], S.L. Korableva[2], B.Z. Malkin[2]

[1] Zavoisky Physical-Technical Institute, FRC Kazan Scientific Center of RAS, Sibirsky trakt 10/7, Kazan 420029, Russia

[2] Kazan Federal University, Kremlevskaya 18, Kazan 420008, Russia

**E-mail: shakurov@kfti.knc.ru*

(Received April 11, 2019; accepted May 7, 2019; published May 16, 2019)

We report the electronic paramagnetic resonance (EPR) studies on single crystals of $LiRF_4$ (R = Y and Lu) doped with Er^{3+} ions in the frequency range of 37-1040 GHz at the liquid helium temperature. Resonance transitions between the Zeeman sublevels of three lower crystal-field Kramers doublets of Er^{3+} ions in magnetic fields up to 1 Tesla are registered. A prominent anisotropy of the EPR spectra in magnetic fields lying in the *ab*-plane of the tetragonal crystal lattice is revealed. The revised set of free-ion and crystal-field parameters for $LiYF_4$:Er^{3+} and the new one for $LiLuF_4$:Er^{3+} allow us to reproduce successfully the measured frequency and angular dependences of the resonant magnetic fields.

PACS: 71.70.Ej,75.10.Dg, 76.30.Kg.

Keywords: crystal field parameters, *g*-factors, magnetic anisotropy, optical spectra.

1. Introduction

The rare-earth doped crystals of double fluorides $LiRF_4$ (R = Y, Lu) are well known model systems in condensed matter physics which are used for different applications in quantum electronics. Additional attention to these compounds was stimulated recently by their applications as quantum memory optical elements. In this case, the detailed information about energies and wave functions of crystal-field states of rare-earth ions is necessary. Traditionally such information about the ground state is obtained from standard electronic paramagnetic resonance (EPR) measurements at low temperatures. To study excited states, one has to work at enhanced temperatures. However, the temperature increasing induces quick relaxation processes and additional broadening of spectral lines that prevents observation of EPR signals. Direct studies of excited states are possible by making use of tunable high frequency EPR technique that allows us to observe resonance transitions from the ground state to excited states at external magnetic fields. In the present work, we carried out high frequency EPR measurements in $LiYF_4$ and $LiLuF_4$ single crystals doped with the trivalent erbium ions.

Rare-earth ions substitute for yttrium or lutetium ions in $LiRF_4$ (R = Y, Lu) crystals at sites with local S_4 symmetry. The ground multiplet $^4I_{15/2}$ of an Er^{3+} ion is split in the tetragonal crystal field to eight Kramers doublets with the wave functions transforming accordingly to irreducible representations Γ_{56} or Γ_{78} of the S_4 point symmetry group. Crystal-field energies of the ground and several excited multiplets of the Er^{3+} ground electronic configuration $4f^{11}$ have been extensively studied by optical spectroscopy [1-3]. In particular, the measured gaps $\Delta_1 = E(\Gamma_{78}^{(1)}) - E(\Gamma_{56}^{(0)})$ and $\Delta_2 = E(\Gamma_{56}^{(2)}) - E(\Gamma_{56}^{(0)})$ between the ground $\Gamma_{56}^{(0)}$ doublet and the first ($\Gamma_{78}^{(1)}$) and the second ($\Gamma_{56}^{(2)}$) excited doublets are represented in Table 1 below. The results of EPR studies of impurity Er^{3+} ions in $LiYF_4$ and $LiLuF_4$ crystals (the measured *g*-factors of the ground and the first excited doublets and the spin-lattice relaxation times) were published in Refs. [4-8]. The most detailed measurements of spectral characteristics of impurity ^{166}Er and ^{167}Er isotopes in the $LiYF_4$ single crystal accompanied by a comprehensive analysis of the data obtained with making use of the high-resolution magneto-optical spectroscopy were published recently in Ref. [9]. However, we found remarkable differences between some results of our measurements and preliminary calculations where we used crystal-field parameters available from literature.

Table 1. Spectral characteristics of impurity Er^{3+} ions in $LiYF_4$ and $LiLuF_4$.

Spectral characteristics	$LiYF_4$		$LiLuF_4$	
	Measured	Calculated	Measured	Calculated
$g_{\parallel}(\Gamma_{56}^{(0)})$	3.137 [4]	3.197	3.096 [7]	3.19
$g_{\perp}(\Gamma_{56}^{(0)})$	8.105 [4]	8.108	8.138 [7]	8.12
Δ_1 (GHz)	517 [1], 510 [8]	510	660 [2], 658*	656.65
$g_{\parallel}(\Gamma_{78}^{(1)})$	8.18 [5], 7.97 [1]	8.109	8.504 [7]	8.50
$g_{\perp}(\Gamma_{78}^{(1)})$	4.43 [5]	4.57	4.302 [7]	4.28
Δ_2 (GHz)	869 [1], 828*	828.6	1050 [2], 1023*	1023.8
$g_{\parallel}(\Gamma_{56}^{(2)})$	0.11 [1], 0.3*	0.19	–	0.20
$g_{\perp}(\Gamma_{56}^{(2)})$	7.8*	7.93	7.9*	7.91

* present work. Absolute values of errors in the measured *g*-factors do not exceed 0.1.

2. Details of experiments and results

We measured EPR spectra within the frequency ν range of 37-1040 GHz at 4.2 K in $LiYF_4$:Er (0.025%) and $LiLuF_4$:Er (0.1%) single crystals grown by Bridgeman-Stockbarger method. The spectra were taken with the wide-band homemade spectrometer equipped by backward wave generators [10] in external magnetic fields up to 1 T. Apart from EPR signals corresponding to intra-doublet transitions, we observed inter-doublet transitions from the Zeeman sublevels of the ground doublet to sublevels of the first and the second excited doublets. Shapes of EPR signals measured at different frequencies in the spectra of $LiRF_4:Er^{3+}$ (R = Y, Lu) are shown in Figure 1.

Let us number the lower six energy levels of Er^{3+} ion in the external magnetic field in ascending order of energy by indices from 1 to 6. The spectral lines corresponding to intra-doublet transitions (see Figure 1a) have a well resolved hyperfine structure (HFS) due to signals from ^{167}Er isotope (natural abundance of 22.9%, nuclear spin $I = 7/2$). Spectral lines corresponding to 2↔3 transitions (Figure 1b) have only partly resolved HFS. It should be noted that the inter-doublet transitions, as compared with the intra-doublet ones, are additionally broadened and have additional fine structure (also observed earlier in Ref. [8]) due to isotopic disorder in the lithium sublattices (crystal-field splittings depend on the relative number of $^6Li^+$ and $^7Li^+$ ions with natural abundances of 7 and 93%, respectively, in the nearest surroundings of an Er^{3+} ion).

The observed EPR signals in $LiLuF_4$ corresponding to the 1↔6 transitions in the magnetic field **B**||**c** (not shown) have weak intensities because of small power of backward wave generators and weak detector (n-InSb) sensitivity at THz frequencies. The measured angular and frequency-field dependences for the inter-doublet transitions in $LiLuF_4:Er^{3+}$ are shown in Figures 2 and 3. The output power of the backward generator depends strongly on frequency, and in the measurements of the

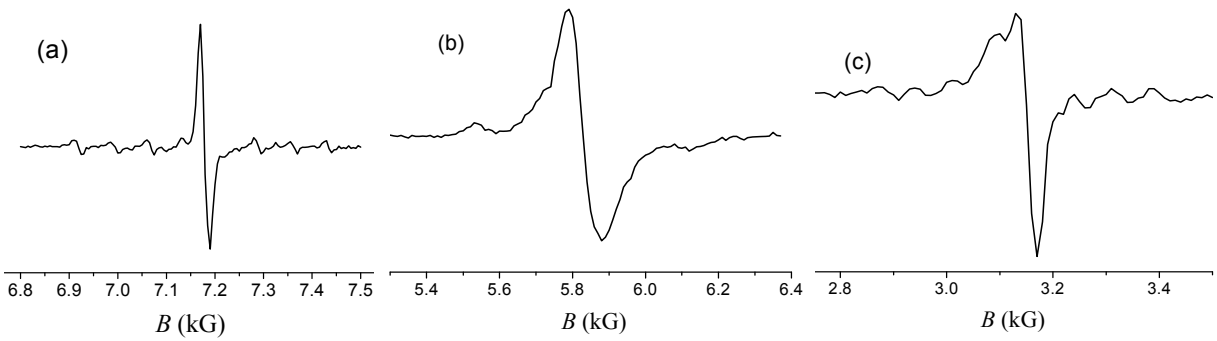

Figure 1. EPR signals in the spectra of $LiLuF_4:Er^{3+}$ (a – 1↔2 transition, $\nu = 82$ GHz, b – 2↔3 transition, $\nu = 603$ GHz) and $LiYF_4:Er^{3+}$ (c – 1↔6 transition, $\nu = 849$ GHz). **B**⊥**c**.

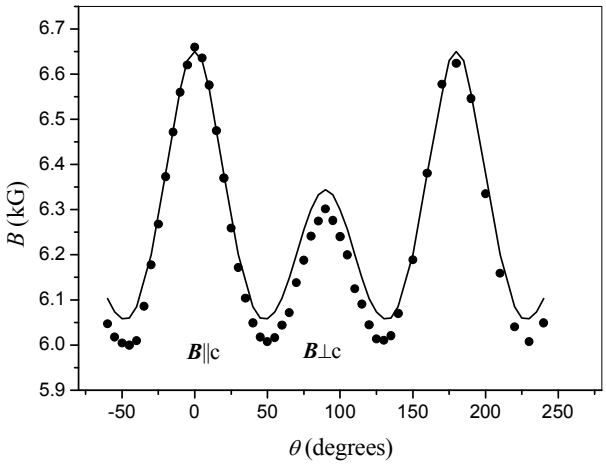

Figure 2. Measured (symbols) and calculated (solid line) angular dependences of the resonant magnetic field in $LiLuF_4:Er^{3+}$ for the 2↔3 transitions at the frequency 603 GHz (θ is the angle between the magnetic field **B** and the *c*-axis in the {010} plane).

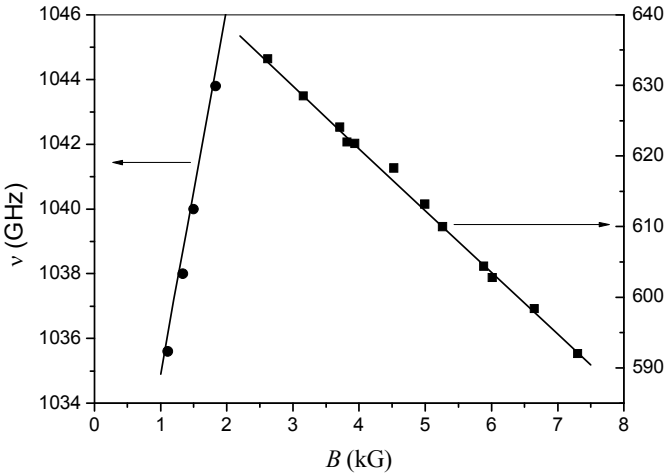

Figure 3. Measured (symbols) and calculated (solid lines) frequency-field dependences for transitions 1↔6 (circles, **B**⊥**c**) and 2↔3 (squares, the magnetic field direction is declined from the *c*-axis by 50 degrees) in $LiLuF_4:Er^{3+}$.

frequency-field dependences we selected the magnetic field orientations corresponding to the largest values of effective *g*-factors and the narrowest spectral lines to improve the signal to noise ratios.

The zero-field splittings (ZFS) $\Delta_1(LiLuF_4) = 658 \pm 1$ GHz and $\Delta_2(LiLuF_4) = 1023$ GHz were determined by making use the linear extrapolations of the measured frequency-field dependences (see Figure 3). It should be noted that it was difficult to register EPR signals corresponding to transitions between the ground $\Gamma_{56}^{(0)}$ doublet and the second excited doublet $\Gamma_{56}^{(2)}$ for magnetic fields **B**||**c** due to small effective *g*-factor, large line width and, correspondingly, small signal to noise ratio. The values of ZFS were additionally checked by comparing the measured and calculated angular dependences of resonant magnetic fields (see below).

The broad band EPR spectra of $LiYF_4:Er^{3+}$ crystals corresponding to resonance transitions from the ground $\Gamma_{56}^{(0)}$ doublet to the first excited $\Gamma_{78}^{(1)}$ doublet have been studied earlier in Ref. [8]. The value of $\Delta_1(LiYF_4) = 510$ GHz has been found. In the present work, we fulfilled detailed measurements of the inter-doublet transitions from the ground doublet to the second excited $\Gamma_{56}^{(2)}$ doublet. The frequency-field dependences for transitions 1↔5, 2↔5, 1↔6 and 2↔6 in the magnetic fields **B**||**c** and **B**⊥**c** are shown in Figure 4. The value of $\Delta_2(LiYF_4) = 828.6 \pm 1$ GHz is obtained directly from measurements in zero magnetic field (see Figure 4). The obtained values of ZFS Δ_1 and Δ_2 agree satisfactorily with the

ones from optical spectroscopy data [1-3], however, the correction for the $\Delta_2(LiLuF_4)$ value (1023 GHz as compared with 1050 GHz [2]) is essential.

Though the measured frequency-field dependences are practically linear, the ascending and descending branches shown in Figure 4 propagate asymmetrically relative to the line $\Delta_2 = 828$ GHz. This asymmetry gives evidence for mutual repulsion of Zeeman sublevels of different crystal-field doublets. Note, the transitions 1↔5 and 2↔6 between the Zeeman sublevels with almost the same magnetic moments (compare $g_\perp(\Gamma_{56}^{(0)})$ and $g_\perp(\Gamma_{56}^{(2)})$ in Table 1) are not observed in the collinear constant and alternating magnetic fields **B**||**B**(*t*) normal to the *c*-axis.

Measurements in the magnetic field **B**⊥**c** while rotating the sample of $LiLuF_4:Er^{3+}$ around the *c*-axis revealed remarkable anisotropy of EPR spectra (see Figure 5a). For different directions of the magnetic field in the *ab*-plane, not only the intensity of EPR signal varies strongly (the mechanism of such a strong intensity variation remains unclear at present time), but the position of the spectral line (a value of the resonant magnetic field) varies as well. Note that the decrease of the signal intensity is accompanied by the increasing asymmetry of the line shape, this brings about an increasing error in the measured line position. The measured angular dependence of the resonant magnetic field in the *ab*-plane is shown in Figure 5b (a similar variation of resonance frequencies in the magnetic field rotating around the S_4 symmetry axis in EPR spectra of $LiYF_4:Er^{3+}$ was marked earlier in Ref. [8]).

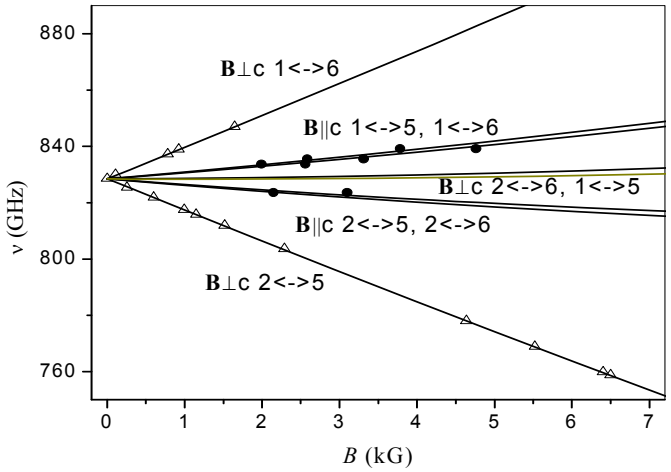

Figure 4. Resonance frequencies vs magnetic fields for the transitions from the ground $\Gamma_{56}^{(0)}$ doublet to the second excited $\Gamma_{56}^{(2)}$ doublet in $LiYF_4:Er^{3+}$. Triangles and circles correspond to transitions in the magnetic fields **B**⊥**c** and **B**||**c**, respectively. The calculated dependences are represented by solid lines.

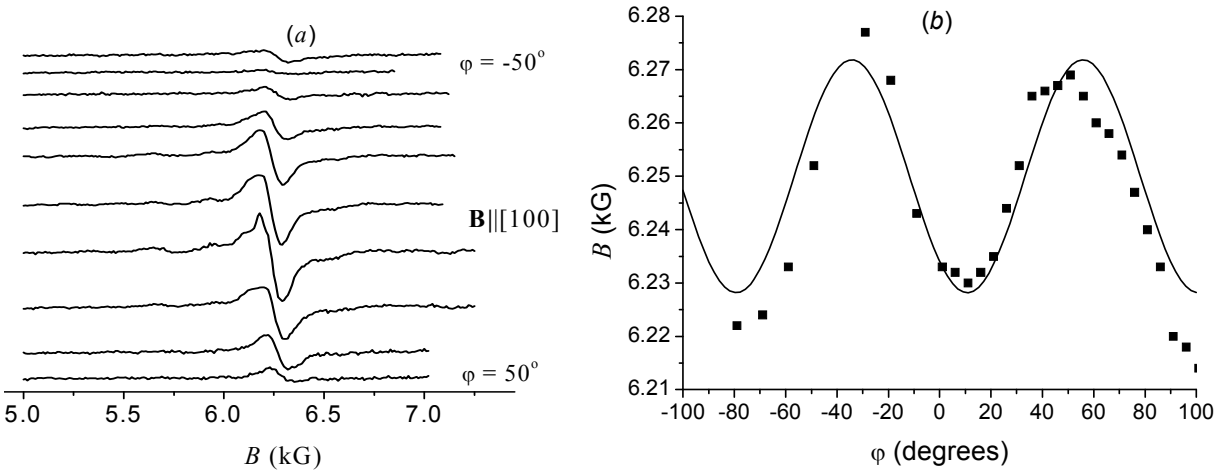

Figure 5. (*a*) EPR signals in $LiLuF_4:Er^{3+}$ for magnetic fields **B** in the (*ab*) plane at the frequency 603 GHz. (*b*) Angular dependence of the resonant magnetic field, φ is the angle between the field and the *a*-axis.

3. Discussion

As has been shown earlier [6], an external magnetic field mixes remarkably wave functions of crystal-field sublevels of the ground multiplet of impurity Er^{3+} ions in $LiYF_4$, and one has to include non-linear in magnetic field terms into the effective Spin-Hamiltonian when describing the EPR spectra corresponding to intra-doublet transitions. In the present work, to analyze the measured frequency-field and angular dependences, we consider the parameterized single-ion Hamiltonian operating in the total space of 364 states of the electronic $4f^{11}$ configuration of an Er^{3+} ion:

$$H = H_{\mathrm{FI}} + H_{\mathrm{CF}} + H_{\mathrm{Z}}, \tag{1}$$

where H_{FI} is the free-ion Hamiltonian written in the standard form [11],

$$H_{\mathrm{FI}} = \sum_{k=2,4,6} F^k f_k + \zeta \sum_n \mathbf{l}_n \mathbf{s}_n + \alpha \mathbf{L}^2 + \beta G(G_2) + \gamma G(R_7) + \sum_{k=2,3,4,6,7,8} T^k t_k + \sum_{k=0,2,4} M^k m_k + \sum_{k=2,4,6} P^k p_k, \tag{2}$$

and the operator H_{CF} determines the crystal-field interaction. In the crystallographic system of coordinates, H_{CF} is written as follows

$$H_{\mathrm{CF}} = \sum_n \left(B_2^0 O_2^0 + B_4^0 O_4^0 + B_4^4 O_4^4 + B_4^{-4} O_4^{-4} + B_6^0 O_6^0 + B_6^4 O_6^4 + B_6^{-4} O_6^{-4} \right), \tag{3}$$

here O_p^k are linear combinations of single-electron spherical tensor operators that coincide with Stevens operators in the truncated space of states of a fixed angular momentum [12]. The operator H_Z corresponds to the Zeeman energy:

$$H_{\mathrm{Z}} = \sum_n \mu_{\mathrm{B}} (k\mathbf{l}_n + 2\mathbf{s}_n)\mathbf{B}. \tag{4}$$

The symbol Σ_n in (2)-(4) means summation over 4f electrons with angular and spin moments, $\mathbf{l}_n$ and $\mathbf{s}_n$, respectively, $k = 0.99$ is the orbital reduction factor. The matrix elements of operators $\mathbf{L} = \Sigma_n \mathbf{l}_n$, $\mathbf{S} = \Sigma_n \mathbf{s}_n$, $\Sigma_n \mathbf{l}_n \mathbf{s}_n$, f_k (the angular parts of the two-electron electrostatic interaction), m_k, p_k (spin-dependent magnetic and relativistic spin-other orbit interactions), t_k (three-body electrostatic interactions) and Casimir operators $G(G_2)$ and $G(R_7)$ in the two-body electrostatic correlation terms in the basis of 364 Slater determinants of the electronic $4f^{11}$ configuration were tabulated by M.V. Vanyunin [13]. Initial values of parameters in (2)-(4) were taken from Ref. [9]. The final set of parameters in the free-ion Hamiltonian (2) (in units of cm^{-1}) for Er^{3+} ions in $LiYF_4$ ($F^2 = 96829$, $F^4 = 68001$, $F^6 = 54342$, $\alpha = 17.1$, $\beta = -582.1$, $\gamma = 1800$, $P^2 = 594$, $P^4 = 297$, $P^6 = 60$, $T^2 = 451$, $T^3 = 61$, $T^4 = 100$, $T^6 = -245$, $T^7 = 305$, $T^8 = 160$, $M^0 = 3.86$, $M^2 = 2.16$, $M^4 = 1.2$, and the spin-orbit coupling constant $\zeta = 2366$) as well as the crystal-field parameters (see Table 2) were determined from the fitting procedure by making use of numerical diagonalization of the Hamiltonian (1) for fixed values and directions of the magnetic field **B** and the subsequent comparison of the measured resonance frequencies with the calculated frequencies of corresponding quantum transitions. The lattice constants of $LiLuF_4$ ($a = 0.5146$ nm, $c = 1.05886$ nm [14]) are slightly less than the ones of $LiYF_4$ ($a = 0.5164$ nm, $c = 1.0741$ nm [15]), and to describe the EPR spectra of Er^{3+} ions in $LiLuF_4$, it was necessary not only to enlarge the crystal-field parameters (see Table 2), but to slightly diminish parameters F^2 and α of the free-ion Hamiltonian (2) as well (for $LiLuF_4$, $F^2 = 96629$ cm^{-1}, $\alpha = 16.9$ cm^{-1}).

The *g*-factors for the Kramers doublets Γ (note, the *g*-tensor has diagonal elements only in the case of local S_4 symmetry) were simulated using the corresponding eigen-functions of the Hamiltonian (1) in zero magnetic field $|\Gamma+\rangle$ and $|\Gamma-\rangle$:

$$g_\perp(\Gamma) = 2\left|\langle\Gamma+|L_x + 2S_x|\Gamma-\rangle\right|, \qquad g_\parallel(\Gamma) = 2\left|\langle\Gamma+|L_z + 2S_z|\Gamma+\rangle\right|.$$

The calculated *g*-factors (see Table 1) as well as the crystal-field splittings of the ground and several excited multiplets (see Table 3) of impurity Er^{3+} ions in $LiYF_4$ and $LiLuF_4$ agree satisfactorily with our experimental data and the available optical data.

Table 2. Crystal-field parameters B_p^k (cm^{-1}).

p	k	$LiYF_4:Er^{3+}$		$LiLuF_4:R^{3+}$	
		[9]	Present work	R = Ho [8]	R = Er Present work
2	0	190	189	188.4	199.0
4	0	−80	−80.1	−80.5	−80.35
4	4	−760.8	−750.3	−640.2	−762.95
4	−4	−679.4	−678.8	−623.6	−690.38
6	0	−2.3	−3.2	−3.5	−3.39
6	4	−363	−378.32	−379.0	−406.82
6	−4	−222	−215.9	−230.3	−214.05

Table 3. Crystal-field energies (cm^{-1}) of the ground and excited multiplet sublevels of Er^{3+} ions.

Doublet symmetry		$LiYF_4$		$LiLuF_4$	
		Experiment	Theory	Experiment [2]	Theory
$^4I_{15/2}$	Γ_{56}	0 [3]	0	0	0
	Γ_{78}	17 [3]	17	22	21.9
	Γ_{56}	27.6 [3]	27.6	35	34.1
	Γ_{78}	56 [3]	58.5	58	64.8
	Γ_{78}	252±2 [1]	245.8	262	257.0
	Γ_{78}	291±6 [1]	288.7	300	304.3
	Γ_{56}	320±3 [1]	316.4	335	330.5
	Γ_{56}	347±3 [1]	344.8	368	363.0
$^4I_{13/2}$	Γ_{78}	6534.3 [3]	6536.5	6545	6544.0
	Γ_{56}	6538.3 [3]	6539.4	6548	6546.6
	Γ_{56}	6578.6 [3]	6579.4	6587	6587.1
	Γ_{78}	6672.5 [3]	6667.5	6684	6677.6
	Γ_{56}	6696.0 [3]	6697.9	6715	6711.3
	Γ_{78}	6724.0 [3]	6719.2	6735	6730.5
	Γ_{56}	6738.3 [3]	6737.0	6750	6750.3
$^4F_{9/2}$	Γ_{78}	15314 [16]	15309	15300	15300
	Γ_{56}	15333 [16]	15334	15327	15327
	Γ_{78}	15349 [16]	15348	15345	15342
	Γ_{78}	15425 [16]	15419	15420	15414
	Γ_{56}	15477 [16]	15474	15450	15471

We obtain also an overall good agreement between the calculated and measured frequency-field dependences (see Figures 3 and 4). Differences between the calculated and measured values (up to 60 G) of resonant magnetic fields in the {010} plane for the 2↔3 transitions (Figure 2) are caused, at least partly, by slightly under-estimated values of $g_\perp$-factors of the ground and the first excited doublets of Er^{3+} ions in $LiLuF_4$; we have also to remember about intrinsic drawbacks of the single-electron crystal-field approach that neglects correlated two-particle terms in H_{CF} and shifts of the crystal-field levels induced by the electron-phonon interaction.

In the case of local S_4 symmetry, the angular dependence of the Zeeman energy of any state of a paramagnetic ion in the external magnetic field **B** lying in the *ab*-plane is described by a four-petal regular rosette. Correspondingly, a frequency of a transition between any two Zeeman sublevels *i* and *j* of Kramers doublets is given by the expression

$$\nu_{ji}(\varphi) = a_{ji}(B) + b_{ji}B^3 \cos[4(\varphi - \varphi_{ji})] \quad (5)$$

where φ is the angle between the magnetic field and the *a*-axis, and functions $a_{ji}(B)$ contain differences of zero-field and Zeeman energies of the considered sublevels. From numerical simulations of the frequencies of the 2↔3 transitions in $LiLuF_4:Er^{3+}$ for different directions of the magnetic field $B = 6.25$ kG in the *ab*-plane, we obtained the following angular dependence of the resonant magnetic field at the frequency of 603 GHz: $B(\varphi) = 6.25 - 0.0218\cos[4(\varphi - 10.8°)]$ (kG). This function matches successfully the experimental data (see Figure 5). Larger absolute values of the measured differences $B(\varphi) - 6.25$ kG in the regions of $\varphi \sim -30°$ and $\varphi \sim +100°$ are most likely caused by a deviation of the rotation axis from the *c*-axis.

The obtained corrected set of crystal-field parameters for impurity Er^{3+} ions in $LiYF_4$ allowed us to reproduce successfully not only the studied in the present work spectral characteristics of the three lower crystal-field sublevels of the ground multiplet $^4I_{15/2}$, but the measured earlier in Ref. [9] *g*-factors of the two lower sublevels of the first excited $^4I_{13/2}$ multiplet and the lowest sublevel of the $^4I_{9/2}$ multiplet as well (see Table 4).

Table 4. *g*-factors of the excited states of Er^{3+} ions in $LiYF_4$.

Energy of the crystal-field doublet (cm^{-1})	$g_\perp$		$g_\parallel$	
	Measured [9]	Calculated	Measured [9]	Calculated
$^4I_{9/2}$ Γ_{78} 12361	2.94	3.00	3.72	3.64
$^4I_{13/2}$ Γ_{56} 6538.3	5.94	5.92	1.30	1.44
$^4I_{13/2}$ Γ_{78} 6534.3	7.32	7.33	1.52	1.53

4. Summary

The obtained sets of crystal-field parameters, the revised one for $LiYF_4:Er^{3+}$ and the new one for $LiLuF_4:Er^{3+}$, can be used for predictions of spectral characteristics of the studied compounds that are necessary for its applications in quantum and optoelectronics.

Acknowledgements

The authors are grateful to V.A. Shustov for X-ray diffraction measurements and orientation of the samples.

References

1. Kulpa S.M. *J. Phys. Chem. Solids* **36**, 1317 (1975)
2. Kaminskii A.A. *Phys. Stat. Sol. A* **97**, K53 (1986)
3. Popova M.N., Chukalina E.P., Malkin B.Z., Saikin S.K. *Phys. Rev. B* **61**, 7421 (2000)
4. Sattler J.P., Nemarich J. *Phys. Rev. B.* **4**, 1 (1971)
5. Antipin A.A., Kazakov B.N., Korableva S.L., Rakhmatullin R.M., Chirkin Yu.K., Fedii A.A. *Izvestia VUZov. Fizika* №9, 93 (1978)
6. Korableva S.L. *Phys. Solid State* **20**, 2139 (1978) [*Fizika Tverdogo Tela* **20**, 3701 (1978)]
7. Abdulsabirov R.Yu., Antipin A.A., Korableva S.L., Rakhmatullin R.M., Rosentsvaig Yu.K. *Izvestia VUZov. Fizika* №2, 24 (1988)
8. Shakurov G.S., Malkin B.Z., Vanyunin M.V., Korableva S.L. *Phys. Solid State* **50**, 1619 (2008)
9. Gerasimov K.I., Minnegaliev M.M., Malkin B.Z., Baibekov E.I., Moiseev S.A. *Phys. Rev. B* **94**, 054429 (2016)
10. Tarasov V.F., Shakurov G.S. *Appl. Magn. Reson*. **2**, 571 (1991)
11. Carnall W.T., Goodman G.L., Rajnak K., Rana S.R. *J. Chem. Phys.* **90**, 3443 (1989)
12. Klekovkina V.V., Zakirov A.R., Malkin B.Z., Kasatkina L.A. *J. Phys.: Conf. Ser.* **324**, 012036 (2011)
13. Vanyunin M.V., *unpublished*
14. Grzechnik A., Friese K., Dmitriev V., Weber H.P., Gesland J.Y., Crichton W.A. *J. Phys.: Condens. Matter* **17**, 763 (2005)
15. Garcia E., Ryan R.R. *Acta Cryst. C* **49**, 2053 (1993)
16. Jayasankar C.K., Reid M.F., Richardson F.S. *Phys. Stat. Sol. B* **155**, 559 (1989)